

Schrödinger's Cat Paradox Revisited: Transfer of Nonclassical Properties from Microscopic Superpositions to Macroscopic Thermal States

H. Jeong and T.C. Ralph

Department of Physics, University of Queensland, St Lucia, Qld 4072, Australia

(Dated: December 2, 2024)

We investigate a more reasonable analogy of Schrödinger's cat paradox, where the state corresponding to the virtual cat is a mixed thermal state with a large average photon number. Several examples show that prominent quantum properties can be transferred from a microscopic superposition to a significantly mixed thermal state. Even when the temperature of the initial thermal state approaches infinity, quantum coherence between extremely mixed thermal states is produced with the maximum negativity of the Wigner functions and conspicuous interference patterns. Entanglement can also be produced under the same condition between extremely mixed thermal states with nearly the maximum Bell-inequality violation.

Can the non-classical properties of the microscopic quantum world be transferred to a macroscopic classical system? It is a fundamental issue in quantum theory to understand the transition mechanism between microscopic quantum systems and macroscopic classical objects. Schrödinger's cat paradox is probably the best known example of a counter-intuitive situation arising from the interaction between quantum and classical worlds [1, 2]. The virtual cat in this paradox is assumed to interact with a microscopic superposition state, $(|g\rangle + |e\rangle)/\sqrt{2}$, where $|g\rangle$ and $|e\rangle$ are the ground and excited states of a two-level atom. The interaction is such that the cat will be dead if the atom is found in the ground state, $|g\rangle$. Thus in Schrödinger's gedanken experiment the cat is supposed to be entangled with the atom as $(|g\rangle|alive\rangle + |e\rangle|dead\rangle)/\sqrt{2}$, where the alive and dead statuses of the cat are described by the state vectors $|alive\rangle$ and $|dead\rangle$. If one measures out the atomic system on the superposed basis the cat will be in a superposition of alive and dead states such as $(|alive\rangle \pm |dead\rangle)/\sqrt{2}$. It is often argued that such entangled states and superposed states can theoretically exist but are virtually impossible to observe because one cannot perfectly isolate a macroscopic object such as the cat from its environment [3].

However, this explanation is not fully satisfactory. In the original gedanken experiment the cat has clearly been interacting with the environment before being placed in the box. The box is then sealed and not opened (measured) till after the interaction between the cat and the atom. Thus a key point is that it is unsatisfactory to describe the "cat" by a pure state such as $|alive\rangle$ and $|dead\rangle$. For example, coherent states with large amplitudes are sometimes regarded as classical pure states and their superposition as a superposition of classical states. However, coherent states are not strictly classical as they cannot be perfectly cloned [4] and display other nonclassical features [5]. These observations naturally lead to the question: if the "cat" in Schrödinger's paradox was in a significantly mixed classical state, how would it be affected by the interaction with a microscopic superposition?

In this paper we investigate this more reasonable anal-

ogy of Schrödinger's paradox, where the "cat" is a significantly mixed thermal state. We first generally consider a two-mode harmonic oscillator system and later discuss its experimental feasibility using current technology. A symmetrically mixed Gaussian state is considered a typically classical state. It approaches a classical probability distribution, which can be well cloned, as its mixedness increases. It was also found that quantum and classical fidelities become identical when the mixedness of two symmetrically mixed states become large [6]. In quantum optics, a thermal state is described by a symmetrically mixed Gaussian state. A displaced thermal state can be defined as $\rho^{th}(V, d) = \int d^2\alpha P^{th}(V, d)|\alpha\rangle\langle\alpha|$ where $|\alpha\rangle$ is a coherent state of amplitude α and

$$P^{th}(V, d) = \frac{2}{\pi(V-1)} \exp\left[-\frac{2|\alpha-d|^2}{V-1}\right]. \quad (1)$$

Suppose that a microscopic superposition state,

$$|\psi\rangle_a = \frac{1}{\sqrt{2}}(|0\rangle_a + |1\rangle_a) \quad (2)$$

where $|0\rangle$ and $|1\rangle$ are the ground and first excited states of the harmonic oscillator, interacts with a thermal state $\rho_b^{th}(V, d)$ and the interaction Hamiltonian is $H_\lambda = \lambda \hat{a}^\dagger \hat{a} \hat{b}^\dagger \hat{b}$ which corresponds to the cross Kerr nonlinearity. The resulting state is then

$$\begin{aligned} \rho_{ab}^{ent} = & \frac{1}{2} \int d^2\alpha P^{th}(V, d) \left\{ |0\rangle\langle 0| \otimes |\alpha\rangle\langle\alpha| \right. \\ & + |1\rangle\langle 0| \otimes |\alpha e^{i\varphi}\rangle\langle\alpha| + |0\rangle\langle 1| \otimes |\alpha\rangle\langle\alpha e^{i\varphi}| \\ & \left. + |1\rangle\langle 1| \otimes |\alpha e^{i\varphi}\rangle\langle\alpha e^{i\varphi}| \right\} \quad (3) \end{aligned}$$

and φ is determined by the strength of the nonlinearity λ and the interaction time. The Wigner representation of ρ_{ab}^{ent} is

$$\begin{aligned} W_{ab}^{ent}(\alpha, \beta) = & \frac{1}{\pi} e^{-2|\alpha|^2} \left\{ W^{th}(\beta; d) + 2\alpha V^c(\beta; d) \right. \\ & \left. + 2[\alpha V^c(\beta; d)]^* + (4|\alpha|^2 - 1)W^{th}(\beta; d e^{i\varphi}) \right\} \quad (4) \end{aligned}$$

where α and β are complex numbers parametrizing the phase spaces of the microscopic and macroscopic systems respectively and

$$W^{th}(\alpha; d) = \frac{2}{\pi V} \exp\left[-\frac{2|\alpha - d|^2}{V}\right], \quad (5)$$

$$V^c(\alpha; d) = \frac{2}{\pi JK} \exp\left[-\frac{2}{K}(1 - e^{i\varphi})d^2 - \frac{1}{J}\left(\alpha - \frac{2e^{i\varphi}d}{K}\right)\left(\alpha^* - \frac{2d}{K}\right)\right], \quad (6)$$

$K = 2 + (V-1)(1 - e^{i\varphi})$, $J = (\sin \varphi + iV \cos \varphi)/(2V \sin \varphi + 2i \cos \varphi)$, and d has been assumed real without loss of generality. If one traces ρ_{ab}^{ent} over mode a , the remaining state will be simply in a classical mixture of two thermal states and its Wigner function will be positive everywhere. However, if one measures out the “microscopic part” on the superposed basis, i.e., $(|0\rangle_a \pm |1\rangle_a)/\sqrt{2}$, the “macroscopic part” for mode b may not lose its nonclassical characteristics. Such a measurement on the superposed basis will reduce the remaining state to

$$\rho^{sup(\pm)} = \mathcal{N}_s^\pm \int d^2\alpha P^{th}(V, d) \left\{ |\alpha\rangle\langle\alpha| \pm |\alpha e^{i\varphi}\rangle\langle\alpha| \pm |\alpha\rangle\langle\alpha e^{i\varphi}| + |\alpha e^{i\varphi}\rangle\langle\alpha e^{i\varphi}| \right\}, \quad (7)$$

where \mathcal{N}_s^\pm are the normalization factors, and its Wigner function is $W^{sup(\pm)}(\alpha) = \mathcal{N}_s^\pm \{W^{th}(\alpha; d) \pm V^c(\alpha; d) \pm \{V^c(\alpha; d)\}^* + W^{th}(\alpha; de^{i\varphi})\}$. The \pm signs correspond to the two possible results from the measurement of the microscopic system. In what follows, we will first address some properties of the two-mode state (3) and then investigate the single-mode state (7) to understand how nonclassical features are transferred from the microscopic superposition to the macroscopic thermal state.

Let us suppose that $\varphi = \pi$. If $V = 1$, the initial state of mode b is a coherent state and Eq. (3) is reduced to entanglement between Fock and pure coherent states such as $(|0\rangle|\alpha\rangle + |1\rangle|-\alpha\rangle)/\sqrt{2}$, where $\alpha = d$, by the Kerr interaction between the two modes. The negativity of the Wigner function is known as an indicator of nonclassicality of quantum states. The maximum negativity of the resulting two-mode Wigner function for $V = 1$ is -0.144 for $d = 0$ and -0.246 for $d \rightarrow \infty$. Now suppose the initial state can be considered a classical thermal state by letting $V \gg 1$. One might expect that the negativity would be washed out as the initial state becomes mixed, but this is not the case. The maximum negativity actually increases as V gets larger. If $V \rightarrow \infty$, the maximum negativity of the Wigner function (4) is -0.246 regardless of d : no matter how mixed the initial thermal state was, the maximum negativity of Wigner function is found to be a large value. The point in the phase space which gives the maximum negativity when $V \gg 1$ or $d \gg 0$ is $(-\frac{1}{2}, 0)$ and has negativity

$$W_{neg} \equiv W_{ab}^{ent}\left(-\frac{1}{2}, 0\right) = \frac{2(-2 + \frac{1}{V} \exp[-\frac{2d^2}{V}])}{\pi^2 \sqrt{e}}. \quad (8)$$

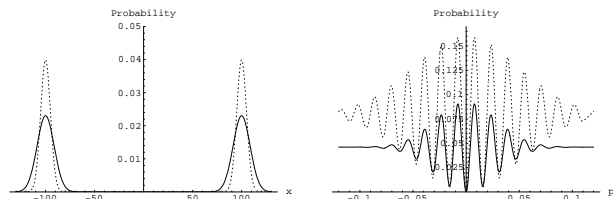


FIG. 1: The probability distributions of x (left) and p (right) for a “superposition” of two distant thermal states. A thermal state with a large mixedness is converted to such a “thermal-state superposition” by interacting with a microscopic superposition (see text). The variance V and displacement d for the thermal state are chosen as $V = 300$ and $d = 100$ (solid line), and $V = 100$ and $d = 100$ (dotted line).

It can be shown that W_{neg} approaches $-4/(\pi^2 \sqrt{e}) \approx -0.246$ when either $d \rightarrow \infty$ or $V \rightarrow \infty$. This unusual effect is obviously due to the interaction between the microscopic superposition and the macroscopic thermal state. If the initial microscopic state is not superposed, e.g., $|\psi\rangle_a = |1\rangle_a$, the resulting state will be a simple direct product, $(|1\rangle\langle 1|)_a \otimes \rho_b^{th}(V, -d)$. Whilst for $V = 1$ this state will exhibit negativity, this is washed out and tends to zero as $V \rightarrow \infty$. Needless to say, if it was $|0\rangle_a$ instead of $|1\rangle_a$, the resulting Wigner function will be a direct product of two Gaussian states whose Wigner function can never be negative. The superposition state (2) plays the crucial role in making the maximum negativity of the resulting Wigner function always saturate to a certain negative value no matter how mixed and classical the initial state of the other mode becomes.

The unusual nonclassical effects become even more prominent with the single-mode state (7). When $\varphi = \pi$ the state (7) becomes $\rho^\pm \propto \rho^{th}(V, d) \pm \sigma(V, d) \pm \sigma(V, -d) + \rho^{th}(V, -d)$, where $\sigma(V, d) = \int d^2\alpha P^{th}(V, d) |\alpha\rangle\langle\alpha|$. If the initial state for mode b is a pure coherent state, i.e., $V = 1$, the measurement on the superposed basis for mode a will produce a superpositions of two pure coherent states as $|\psi_\pm\rangle \propto |\alpha\rangle \pm |-\alpha\rangle$. Note that the maximum negative value of the Wigner function for the state $|\psi_-\rangle$ is always $-2/\pi$ (≈ -0.637) while the corresponding value approaches $-2/\pi$ as $d \rightarrow \infty$ for the case of $|\psi_+\rangle$. This value, $-2/\pi$, is the maximum negativity that can be exhibited by a Wigner function. Again, one might expect this negativity to be reduced by mixing of the initial state but this is not the case. The maximum negative value of the Wigner function of ρ_- is always $-2/\pi$ regardless of V and d . Meanwhile, the maximum negative value of the Wigner function for ρ_+ approaches $-2/\pi$ as d gets large. The probability \mathcal{P}_\pm to obtain the state ρ^\pm is $\mathcal{P}_\pm = (1 \pm \exp[-2d^2/V])/2$.

Suppose that both V and d are very large for the initial thermal state. As we have discussed earlier, our examples may become more reasonable analogies of Schrödinger’s paradox in this limit. Note that two thermal states $\rho^{th}(V, \pm d)$ become macroscopically distinguishable when $d \gg \sqrt{V}$. We have found that both the states ρ^\pm in

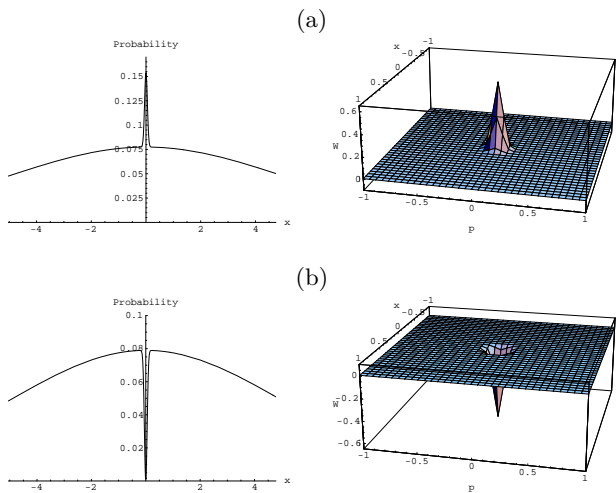


FIG. 2: The probability distributions (left) and Wigner functions (right) of the thermal state of $V = 100$ around the origin ($d = 1$) after an interaction with a microscopic superposition and a conditional measurement.

this case show probability distributions with two Gaussian peaks and interference fringes. Fig. 1 presents the probability distributions of x ($\equiv \text{Re}[\alpha]$) and p ($\equiv \text{Im}[\alpha]$) for ρ^- when $V = 300$ and $d = 100$ (solid line) and when $V = 100$ and $d = 100$ (dotted line). The probability distribution of x (p) for ρ^\pm can be obtained by integrating the Wigner function of ρ^\pm over p (x). The two Gaussian peaks along the x axis and interference fringes along the p axis is a typical signature of a quantum superposition between macroscopically distinguishable states. The high visibility of the fringes is incompatible with classical physics. We emphasize that such a state is a “superposition” of severely mixed thermal states exhibiting maximum Wigner function negativity of $-2/\pi$.

When d is small while V is still very large, i.e., a classical thermal state around the origin is assumed as the initial state, the resulting states also show very peculiar nonclassical behaviors. Fig. 2 shows the probability distribution and the Wigner functions of the states ρ^\pm where $V = 100$ and $d = 1$. As a result of the interaction with the microscopic superposition, a deep hole has been formed around the origin for ρ^- (or a sharp pole toward the top for the case of ρ^+). While the maximum negative value of the Wigner function of ρ^- is $-2/\pi$ regardless of the value of V , the volume of the negativity decreases as V gets larger. Therefore the hole at the origin looks like a needle in Fig. 2(b). In this case, however, the probability \mathcal{P}_- is only 1% while \mathcal{P}_+ is 99%.

We now consider what will happen when φ , V and d take moderate values, which may be more experimentally practical. When $V = 4$, $d = 4$ and $\varphi = \pi/4$, the resulting state shows interference fringe as shown in Fig. 3. The maximum negativity of the Wigner function in this case is -0.118 . Fig. 4 shows the situation for $V = 100$, $d = 0$ and $\varphi = \pi/16$, i.e., the thermal state of a large variance at origin and only small amount of rotation by

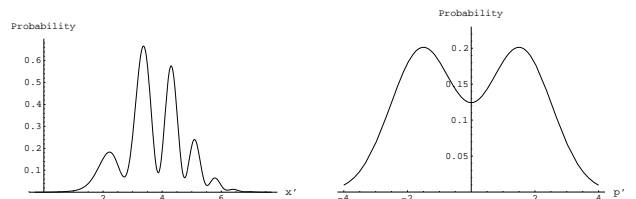


FIG. 3: The probability distributions of x (left) and p (right) for a “superposition” of thermal states where $V = 4$, $d = 4$, $\varphi = \pi/4$. The interference fringe is evident and the maximum negativity of the Wigner function is ≈ -0.12 . The x' (p') axis in this figure has been rotated by $\pi/8$ from the x (p) axis for clarity.

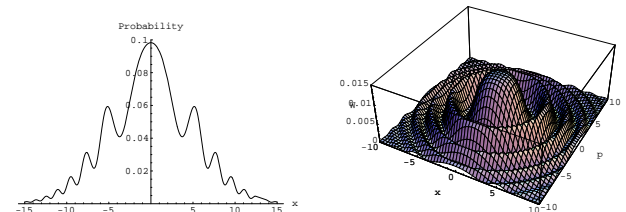


FIG. 4: The probability distribution (left) and the Wigner function (right) of the thermal state of the variance $V = 100$ at origin after weakly interacting with a microscopic superposition ($\varphi = \pi/16$).

the interaction. Note that this case is deterministic because $\mathcal{P}_- = 0$ for $d = 0$. It is interesting to observe that only a small amount of φ makes a thermal state a non-Gaussian pattern shown in Fig. 4. If it was a vacuum coherent state, i.e., $V = 1$, the state would have remained a vacuum state.

We have examined the negativity of the Wigner function and interference fringes of the superposition of the mixed thermal states. Another important question concerns the possibility of generating entanglement between macroscopic objects and its Bell-type inequality tests [7]. Recently, the possibility of generating macroscopic entanglement in the classical limit have been studied [11]. In our approach, such macroscopic entanglement can be naturally generated *between* very large thermal states and verified as follows. If the microscopic superposition interacts with two thermal states, $\rho_b^{th}(V, d)$ and $\rho_c^{th}(V, -d)$, and the microscopic particle is measured out on the superposed basis [12], the resulting state will be

$$\rho^{tm(\pm)} \propto \rho^{th}(V, d) \otimes \rho^{th}(V, -d) \pm \sigma(V, d) \otimes \sigma(V, -d) \pm \sigma(V, -d) \otimes \sigma(V, d) + \rho^{th}(V, -d) \otimes \rho^{th}(V, d). \quad (9)$$

Thermal fields in two cavities and a two-level atom can be used to generate such a state. Here we shall consider the Bell-CHSH inequality [7, 8] with photon number parity measurements [12, 13]. Such parity measurements can be made in a high-Q cavity using a far-off-resonant interaction between a two-level atom and the field [14]. It can be simply shown that the maximum negativity of the Wigner function for $\rho^{tm(-)}$ is $-4/\pi^2 \approx -0.405$, at

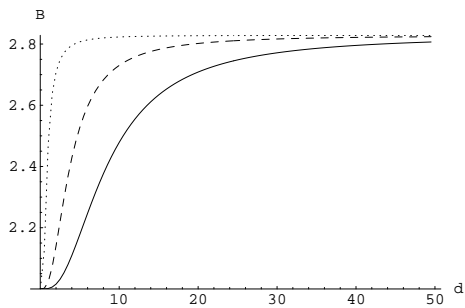


FIG. 5: The maximum violation B of Bell-CHSH inequality for the “thermal-state entanglement”, ρ_+ , of $V = 100$ (solid line) and $V = 20$ (dashed line). The Bell-violation of a pure entangled coherent state, i.e., $V = 1$, has been plotted for comparison (dotted line).

the origin regardless of the values of V and d . This value is again the maximum negativity that can be exhibited by a two-mode Wigner function. As shown in Fig. 5, the Bell-violation approaches the maximum value for a bipartite measurement, $2\sqrt{2}$ [9], when $d \gg 1$ regardless of the level of the mixedness V . Note that it is true for both of ρ_+ and ρ_- even though only the case of ρ_+ has been plotted in Fig. 5. This implies that entanglement of nearly 1 ebit has been produced between the two significantly mixed thermal states for $d \gg 0$, and such “thermal-state entanglement” cannot be described by a local theory. A fundamental question, which is beyond the scope of this paper, might be “Can homodyne detection (i.e. a classical measurement) be used to see a Bell-inequality violation of such states?”

We now address experimental feasibility of our examples. Probably the most feasible experimental setup to test our examples is atom-field interactions in cavities where a $\pi/2$ pulse can be used to prepare the atom in a superposed state. This type of experiment has already been performed to produce a superposition of coherent states [10]. In our cases, simply thermal states can be

used instead of coherent states. Of course, the interaction for $\varphi = \pi$ is a highly demanding requirement. However, states such as shown in Figs. 3 and 4, where φ and d take moderate values, would be in the scope of experiment realization using current technology. The two-mode thermal-state entanglement can also be generated using two cavities and an atomic state detector [12]. Another possible setup is an all-optical scheme with free-traveling fields and a cross-Kerr medium, where a single photon source and a single rail quantum gate [15] could be used to generate the microscopic superposition. Recently, there have been theoretical and experimental efforts to produce and observe giant Kerr nonlinearities using electromagnetically induced transparency [16]. Two-mode entanglement in a traveling field configuration can be produced at a 50-50 beam splitter. It should be noted that the coherence time of such macroscopic mixed quantum states will become shorter as d gets larger [17], i.e., interactions with environments *after* interacting with the microscopic system will rapidly destroy the quantum effects.

We have studied a more reasonable analogy of Schrödinger’s cat paradox where the virtual cat is a significantly mixed thermal state. Our discussion was motivated by the observation that a truly classical system cannot be in a pure quantum state. We have found that non-classical properties of microscopic quantum superpositions can be transferred to thermal states of large average photon numbers. The resulting states show strong quantum coherence and entanglement between severely mixed thermal states. Our examples are feasible in real physical systems and may be realized for some moderate cases using current technology. Finally, it will be an interesting future work to explore the possibility of quantum information processing using the thermal-state “superpositions” and entanglement studied in this paper.

This work was supported by the Australian Research Council. H.J. thanks M.S. Kim for useful discussions.

-
- [1] E. Schrödinger, *Naturwissenschaften*. **23**, pp. 807-812; 823-828; 844-849 (1935).
[2] A.J. Leggett and A. Garg, *Phys. Rev. Lett.* **54**, 857 (1985); M.D. Reid, quant-ph/0101062 and references therein.
[3] J. Preskill, Lecture Note on Quantum Computation, www.theory.caltech.edu/people/preskill/ph229 (1999); M.A. Nielsen and I.L. Chuang, *Quantum Computation and Quantum Information*, Cambridge (2000).
[4] W.K. Wootters and W.H. Zurek, *Nature (London)* **299**, 802 (1982).
[5] L.M. Johansen, *Phys. Lett. A* **329**, 184.
[6] H. Jeong, T.C. Ralph, and W.P. Bowen, quant-ph/0409101.
[7] S. Bell, *Physics* **1**, 195 (1964).
[8] J.F. Clauser *et al.*, *Phys. Rev. Lett.* **23**, 880 (1969).
[9] B.S. Cirel’son, *Lett. Math. Phys.* **4**, 93 (1980).
[10] Q.A. Turchette *et al.*, *Phys. Rev. Lett.* **75**, 4710 (1995); M. Brune *et al.*, *Phys. Rev. Lett.* **77**, 4887 (1996); A. Auffeves *et al.*, *Phys. Rev. Lett.* **91** 230405 (2003).
[11] M.C. Arnesen, S. Bose, and V. Vedral *Phys. Rev. Lett.* **87**, 017901 (2001); S. Bose *et al.*, *Phys. Rev. Lett.* **87**, 050401 (2001); V. Vedral, *New J. Phys.* **6** 102 (2004); C. Brukner and V. Vedral, quant-ph/0406040 and reference therein; M.J. Everitt *et al.*, quant-ph/0409112.
[12] M.S. Kim and J. Lee, *Phys. Rev. A* **61** 042102 (2000).
[13] K. Banaszek and K. Wódkiewicz, *Phys. Rev. A* **58**, 4345 (1998); *Phys. Rev. Lett.* **99**, 2009 (1999).
[14] B.-G. Englert, N. Sterpi, and H. Walther, *Opt. Commun.* **100** 526 (1993).
[15] A.P. Lund and T.C. Ralph, *Phys. Rev. A* **66**, 032307 (2002).

- [16] H. Schmidt and A. Imamoglu, *Opt. Lett.* **21**, 1936 (1996);
L.V. Hau *et al.*, *Nature* **397**, 594 (1999).
- [17] W. H. Zurek, *Physics Today* **46**(4), 13, 81 (1993).